ELSEVIER

Journal of Crystal Growth 180 (1997) 433–441

JOURNAL OF CRYSTAL GROWTH

Unsteady three-dimensional buoyancy-driven convection in a circular cylindrical cavity and its damping by magnetic field

H. Ben Hadid*, D. Henry, R. Touihri

Laboratoire de Mécanique des Fluides et d'Acoustique, UMR 5509, Ecole Centrale de Lyon, Université Claude Bernard Lyon 1, BP 163, F-69131 Ecully Cedex, France

Abstract

The oscillatory convection in an electrically conducting liquid-metal confined in a cylindrical cavity of moderate length is investigated using a spectral numerical method involving direct resolution of the Navier–Stokes equations for three-dimensional flows. Time signals, symmetry properties and energy budgets are presented in order to characterize the flow oscillations. The damping of the oscillatory flows by a vertical magnetic field is then studied up to the stabilization to a steady flow.

1. Introduction

The quality of crystals grown from melts is determined largely by their homogeneity of composition and structure. All crystal growth processes of solidification from a melt involve temperature gradients; these temperature gradients cause density gradients, which can lead to natural convection when a gravity field is present. Convection in the molten metal is typically vigorous and affects the heat transfer, the mixing of solutes, and ultimately the microstructure of the finished product. A problem occurs when the flow is oscillatory; this can result in periodic conditions of growth and thus periodic inhomogeneities in the crystals. Experimental studies have been carried out to identify the conditions for the appearance of such oscillations [1–4]. It has been shown that thermal oscillations appear spontaneously beyond a critical threshold even in the absence of solidification. These thresholds have been calculated by theoretical approaches in different simplified configurations [5–7], but only few results are available in more realistic confined three-dimensional situations [8].

When a magnetic field is applied to an electrically conducting liquid, the liquid motion is reduced because of the interaction between the imposed magnetic field and the induced electric current [9–11]. Therefore, the use of a magnetic field is considered to be an effective means for reducing or eliminating the undesired effects due to flow oscillations in electrically conducting liquids. This potentiality has been shown experimentally [12], but has not been much explored by theoretical and numerical studies [13].

* Corresponding author. Fax: + 33 4 78647145; e-mail: benhadid@mecaflu.ec-lyon.fr.

PII S0022-0248(97)00291-1

In this paper, we investigate the unsteady three-dimensional buoyancy-driven flows appearing in a moderate length cylindrical cavity corresponding to the horizontal Bridgman configuration. Symmetry considerations, spectral analyses and energy budgets are used to characterize the observed unsteady flows. A constant vertical magnetic field is then applied to the system, and the damping of the flow oscillations is analysed up to stabilization.

2. Mathematical model

We consider a cylindrical cavity of aspect ratio $A = L/D$ (where D is the diameter and L the length of the cavity, see Fig. 1) filled with an electrically conducting liquid metal submitted to a horizontal temperature gradient which generates a laminar convective motion. A vertical magnetic field can be applied to the system.

The basic equations used in the simulations of the melt flow are the Navier–Stokes equations including the Lorentz force and using the Boussinesq approximation for buoyancy, since the metallic liquid is considered incompressible. The three-dimensional conservation equations of momentum and energy are made dimensionless using D, D^2/ν, $U_{\mathrm{ref}} = \mathrm{Gr}^{1/2}\nu/D$, $\Delta\tilde{T}/A$, $\boldsymbol{B}_0$ and $\sigma_e U_{\mathrm{ref}} \boldsymbol{B}_0$ as scales for length, time, velocity, temperature, magnetic flux density and electric current density, respectively (ν is the kinematic viscosity, σ_e the electric conductivity and $\Delta\tilde{T} = \tilde{T}_h - \tilde{T}_c$ is the difference of temperature between the vertical endwalls, $\tilde{T}_h$ being imposed at the hot right endwall and $\tilde{T}_c$ at the cold left endwall). Using these nondimensionalizations, the governing equations in the melt may be written as

$$\nabla \cdot \boldsymbol{v} = 0, \tag{1}$$

$$\frac{\partial \boldsymbol{v}}{\partial t} + \mathrm{Gr}^{1/2}(\boldsymbol{v}\cdot\nabla)\boldsymbol{v} = -\nabla p + \nabla^2 \boldsymbol{v} + \mathrm{Gr}^{1/2} T \boldsymbol{e}_y + \mathrm{Ha}^2 \boldsymbol{J} \times \boldsymbol{e}_y, \tag{2}$$

$$\frac{\partial T}{\partial t} + \mathrm{Gr}^{1/2}(\boldsymbol{v}\cdot\nabla T) = \frac{1}{\mathrm{Pr}}\nabla^2 T, \tag{3}$$

where $\boldsymbol{v}$, p and T are the dimensionless velocity field ($\boldsymbol{v} = (u,v,w)$), pressure and temperature respectively. T is defined as $T = A(\tilde{T} - \tilde{T}_m)/\Delta\tilde{T}$ where $\tilde{T}_m$ is the mean temperature in the cavity. The magnetic flux density vector $\boldsymbol{B}$ in the Lorentz force is set equal to $\boldsymbol{B}_0$ (the uniform applied field) as the induced field

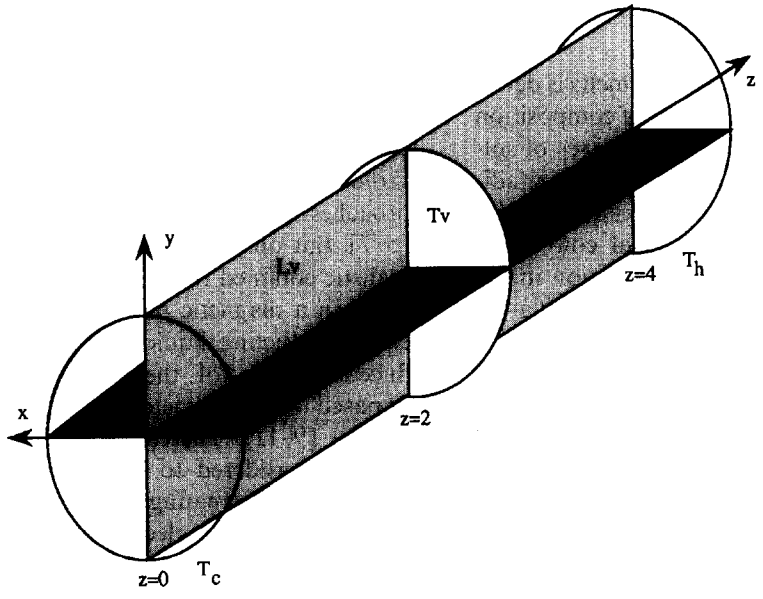

Fig. 1. Geometry of the cylindrical cavity and of the reference frame.

$\boldsymbol{b}$ is small ($Re_m \ll 1$, where Re_m is the magnetic Reynolds number). The dimensionless electric current density $\boldsymbol{J}$ is given by Ohm's law for a moving fluid:

$$\boldsymbol{J} = \boldsymbol{E} + \boldsymbol{v} \times \boldsymbol{e}_y, \tag{4}$$

where $\boldsymbol{E}$ is the dimensionless electric field. Here, since $Re_m \ll 1$, the electric field can be written as the gradient of an electric potential ($\boldsymbol{E} = -\nabla\phi$). The equation of continuity for electric current density gives

$$\nabla \cdot \boldsymbol{J} = 0, \tag{5}$$

which, combined with (4), leads to

$$\nabla^2\phi = \boldsymbol{e}_y \cdot (\nabla \times \boldsymbol{v}). \tag{6}$$

The boundary conditions for the velocity are the usual no-slip conditions $u = v = w = 0$ on all the walls. Adiabatic conditions are chosen for the temperature along the lateral wall. For the electric current density $\boldsymbol{J}$, insulated conditions $\boldsymbol{J} \cdot \boldsymbol{n} = 0$ are adopted on all the boundaries. The dimensionless parameters appearing in Eqs. (1)–(3) are the Grashof number $Gr = g\beta\Delta\tilde{T}D^4/Lv^2$, the Prandtl number $Pr = v/\kappa$ and the Hartmann number $Ha = \boldsymbol{B}_0 D\sqrt{\sigma_e/\rho v}$, where β is the coefficient of volumetric expansion, g the gravity constant, ρ the fluid density and κ the thermal diffusivity.

The numerical simulations are performed in a cylindrical cavity of moderate aspect ratio ($A = 2.5$ or 3) for a Prandtl number equal to 0.026, a value corresponding to experiments with mercury [12]. The spatial discretization of the governing Eqs. (1)–(6) is based on an isoparametric spectral element method [14] which is a high-order weighted residual technique. The cylindrical geometry is divided into five subdomains; in each one $9 \times 9 \times 35$ (following x, y and z, respectively) Gauss-Lobatto-Legendre collocation points were used. The time-discretization of Eqs. (2) and (3) employs a high-order time-difference scheme combined with a splitting algorithm [15]. We need to define different planes inside the circular cylinder in order to characterize the results (Fig. 1): the (Lv)-plane (longitudinal vertical middle plane, main plane of circulation), the (Lh)-plane (longitudinal horizontal middle plane), and the (Tv)-plane (transverse vertical middle plane).

3. Oscillatory flows in a moderate length cavity

The transition to oscillatory flow is studied without magnetic field for a cylindrical cavity of moderate length ($A = 2.5$ or 3). In such a cavity, the steady flow verifies all the original symmetries of the problem, namely a reflexion symmetry (Sp) with respect to the (Lv)-plane and a reflexion symmetry (Sa) with respect to the (Th)-axis (transverse horizontal centre axis). The combination of these two symmetries also gives a symmetry (Sc) with respect to the centre point of the cavity. This steady flow evolves, when Gr is increased, through the appearance of pseudo-recirculations in the end regions inside the large convective loop. In moderate length cavities, these recirculations interact near the centre of the cavity where a kind of stagnation zone appears.

The transition to time-dependent flow occurs under the form of a Hopf bifurcation for a critical value of the Grashof number, Gr_c, around $Gr_c = 149\,500$ for $A = 2.5$ and $Gr_c = 143\,000$ for $A = 3$. These transition values have been obtained by successive simulations on both sides of the thresholds, where the upper side corresponds to increasing oscillatory signal and the lower side corresponds to a decreasing signal, with interpolation to zero growth rate. Further calculations beyond the thresholds have been performed, up to $Gr = 230\,000$ for $A = 3$ ($(Gr - Gr_c)/Gr_c = 61\%$).

The instability which develops in moderate length cavities seems to be connected to the interaction at the centre of the cavity between the end recirculations. The instability corresponds spatially to a breaking of the longitudinal symmetries, the (Sa) and (Sc) symmetries, but keeps the (Sp) symmetry, which concerns the transverse direction (Fig. 2). The time series obtained close to the threshold show very regular oscillations with a single frequency f_0 (hereafter referred to as the fundamental frequency) around 50. The signal becomes quickly more complex as Gr is increased with the appearance of harmonics (see the time series obtained on the dimensionless temperature at the

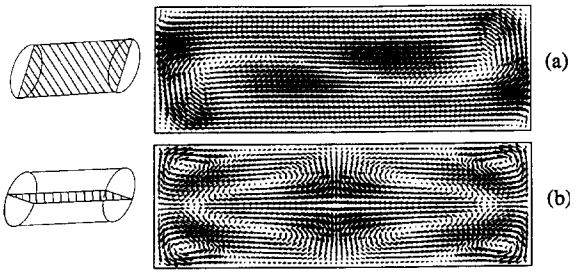

Fig. 2. Instantaneous velocity vectors in the (Lv)-plane (a) and in the (Lh)-plane (b) for an oscillatory situation; $Gr = 1.5 \times 10^5$ and $A = 3$.

point ($x = 0, y = 0.25, z = 1.5$) in Fig. 3 for $A = 3$). We may note at $Gr = 150000$ the presence of a very low frequency which corresponds to a kind of intermittency. This intermittency, particularly well visible in the time series measured on the temperature, seems to be connected to the change of the position of the stagnation zone, which is located for a while on the right side of the central (Th)-axis when the left recirculation is stronger, and then on the other side. A further increase of Gr leads to more chaotic signals with amplification of the harmonics. The fundamental frequency f_0, which was around 50 at the transition, is shifted towards higher frequencies as Gr is increased, $f_0 = 61.36$, 72.17 and 87.24 for $Gr = 175000$, 200000 and 230000 respectively. Note that the time series and power spectra given in Fig. 3, which have been chosen to illustrate the intermittency phenomenon, do not clearly show the fundamental frequencies.

To show the positions of the zones which are affected by the basic oscillations, we have calculated the spatial dependence of the power spectral density $\hat{T}$ for the temperature signal, defined by

$$\hat{T}(x, y, z, f_0) = \int_t T(x, y, z, t) e^{-i(2\pi t f_0)} \, dt$$

and based on the correlation between the signal of T and the fundamental periodic signal with frequency f_0. The results, presented in Fig. 4 by means of cross-sections in the (Lv) and (Lh)-planes, show that these zones are located along the line of shear between the opposite flows, while being limited to the vicinity of the (Lv)-plane. In this figure, the contribution is stronger on the right side of the cavity, because the time-averaged values have been calculated over a time interval where the right recirculation was dominant.

To acquire more insight into the problem, we have performed a fluctuating kinetic energy analysis for the oscillatory situation close to the threshold. Results are presented for the cavity with $A = 2.5$ at $Gr = 150000$. We define the fluctuating kinetic energy as

$$k = u_i' u_i'/2,$$

where u_i' represents the fluctuating velocity components such that

$$u_i(x, y, z, t) = \bar{u}_i(x, y, z) + u_i'(x, y, z, t),$$

where

$$\bar{u}_i(x, y, z) = \lim_{t^* \to \infty} \frac{1}{t^*} \int_{-t^*/2}^{t^*/2} u_i(x, y, z, t) \, dt$$

is the time averaged mean value. In Fig. 5, the rate of change of the kinetic energy $\partial k/\partial t$ during a fundamental period is given through snapshots of the spatial distribution. The production zones correspond to dark colours and the dissipation zones to light colours. These production and dissipation zones are found along a curved line which is the border between opposite direction flows (see Fig. 2a). In fact, they are created near the centre of the cavity through alternate pairs of production and dissipation zones. These zones are transported by the flow from the centre to the end walls, first growing and then decreasing to finally disappear at the end walls. Within each pair of simultaneously created zones the zone initiated at the right of the flow centre point is moved towards the right and the zone initiated at the left of this point is moved towards the left. It can also be mentioned that the zones located in the left part of the cavity have globally a stronger intensity than the zones located in the right part: this has to be connected with the fact that the elementary period has been chosen during an intermittent sequence for which the left recirculation is stronger. The same type of behaviour is obtained for $\partial\theta/\partial t$, the rate of change of the thermal energy ($\theta = T'^2/2$ where T' is the

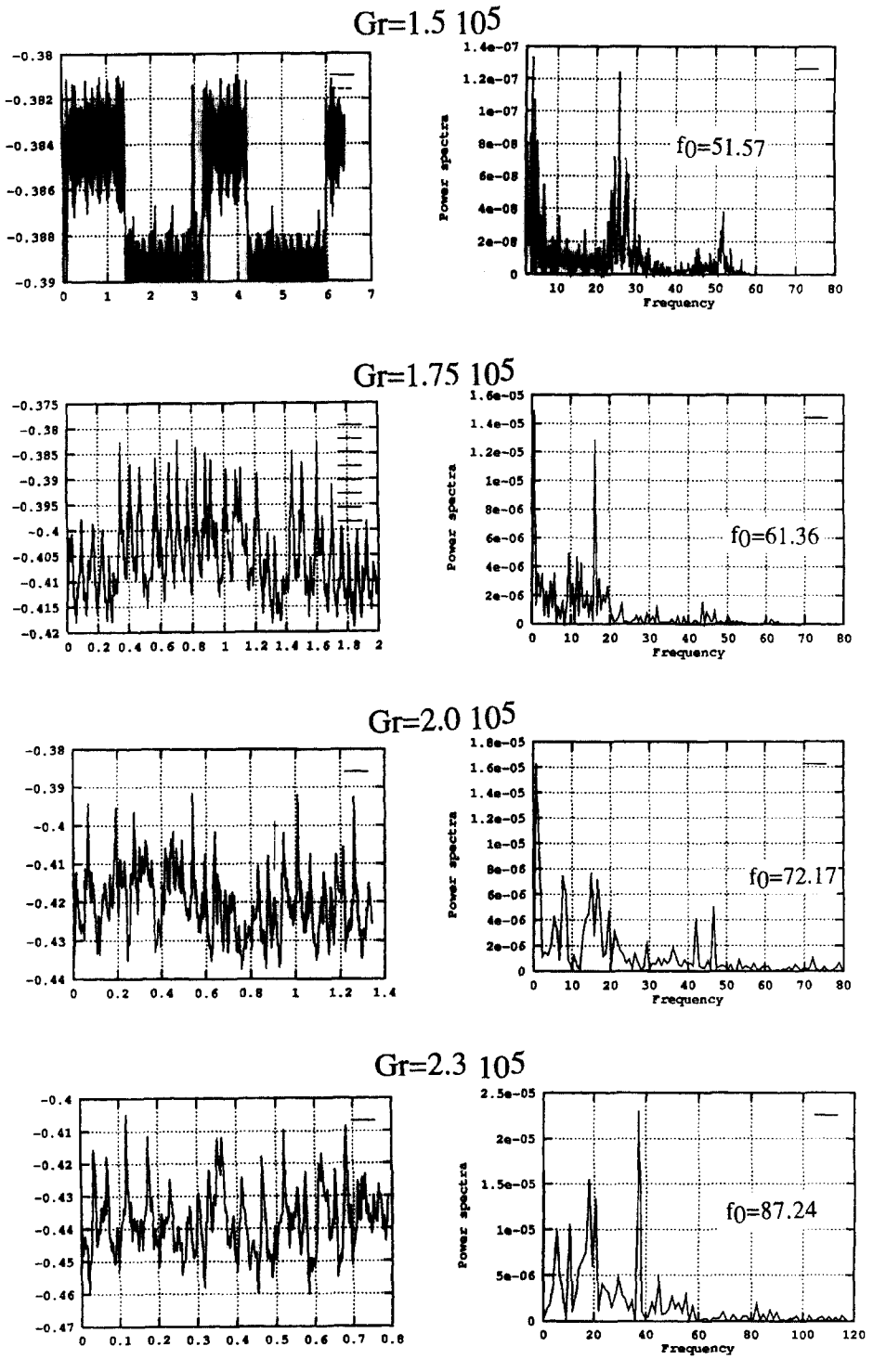

Fig. 3. Time series (left) and power spectra (right) of the dimensionless temperature T at point ($x = 0$, $y = 0.25$, $z = 1.5$) for different Gr ($A = 3$). The power spectra are expressed using the square of the amplitudes.

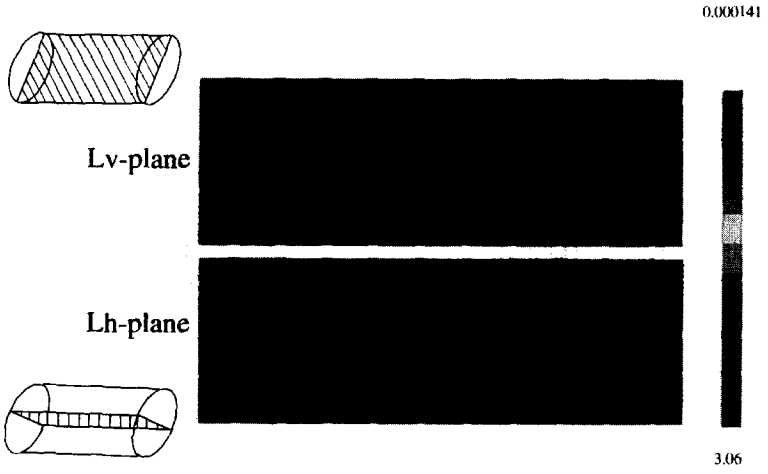

Fig. 4. Spatial dependence of the power spectral density calculated on the temperature signal, $\hat{T}$: views in the (Lv) and (Lh)-plane, $Gr = 1.5 \times 10^5$ and $A = 3$.

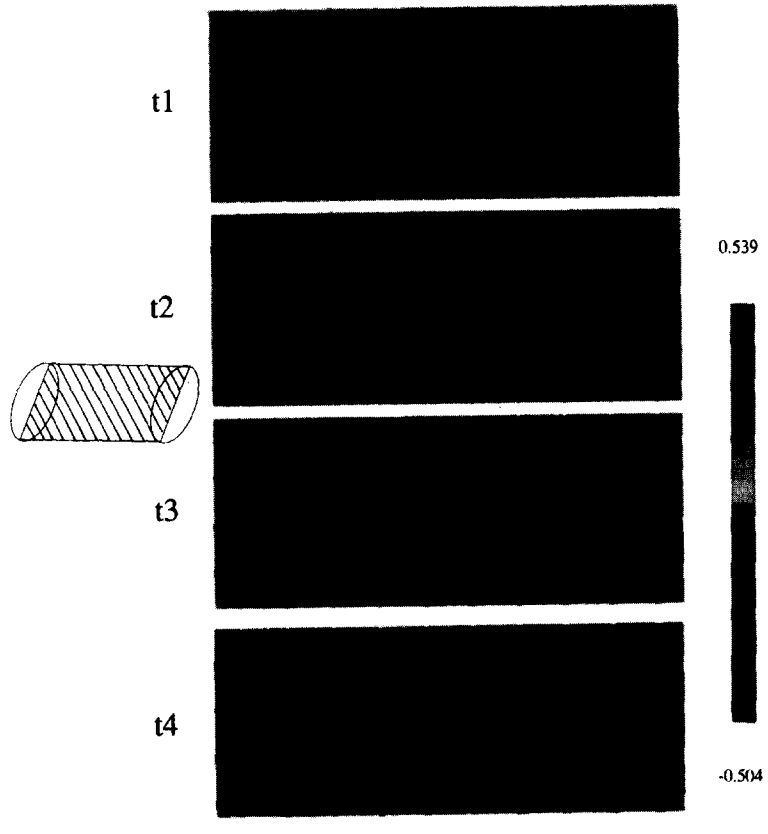

Fig. 5. Snapshots of the distribution of the rate of change of the kinetic energy $\partial k/\partial t$ during a fundamental period: $Gr = 1.5 \times 10^5$ and $A = 2.5$.

fluctuating temperature), but the levels are at least two orders of magnitude smaller than for the kinetic energy.

Finally, the importance of the different contributions to the fluctuating kinetic energy has been determined by calculating the evolution of the rate of change of the total fluctuating kinetic energy K, i.e., the kinetic energy integrated over the whole volume of the cavity. We can write

$$\frac{\partial K}{\partial t} = \frac{\partial}{\partial t}\left(\int_\Omega k \, d\Omega\right) = Ec_{ps} + Ec_{dv} + Ec_{buoy},$$

where

$$Ec_{ps} = -\mathrm{Gr}^{1/2}\int_\Omega u_i' u_j' \frac{\partial \bar{u}_i}{\partial x_j} \, d\Omega$$

{Production of fluctuating kinetic energy by shear of meanflow}

$$Ec_{dv} = -\int_\Omega \left(\frac{\partial u_i'}{\partial x_j}\right)^2 d\Omega$$

{Viscous dissipation of fluctuating kinetic energy}

$$Ec_{buoy} = \mathrm{Gr}^{1/2}\int_\Omega u_i' T' \delta_{i2} \, d\Omega$$

{Production of fluctuating kinetic energy by buoyancy forces}

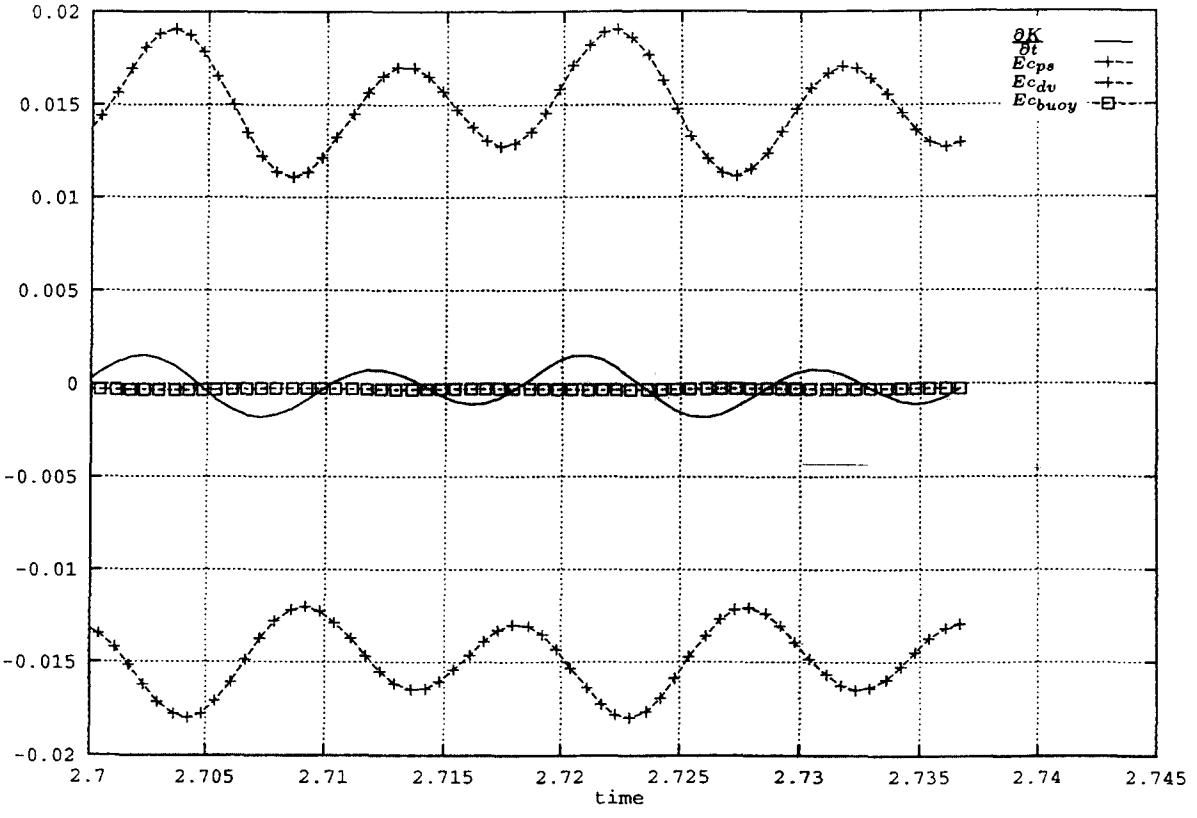

Fig. 6. Time evolution of the rate of change of the total fluctuating kinetic energy $\partial K/\partial t$ together with the main contributions; $\mathrm{Gr} = 1.5 \times 10^5$ and $A = 2.5$.

In Fig. 6 (still at Gr = 150 000 for $A = 2.5$), we can see that the main contribution is the production Ec_{ps} by shear of the mean flow, while a strong dissipation Ec_{dv} is due to viscosity, whereas the contribution from the buoyancy forces Ec_{buoy} is much less important. The budget of the total fluctuating thermal energy Θ has also been evaluated but, as expected, the level of the contributions is much smaller than for the kinetic energy.

All these results show that the oscillatory instability obtained in such cavities is connected to shear through the creation of perturbations created in the core region along the surface separating the upper and lower reverse flows. These perturbations are then transported by the flow towards the end walls where they are damped.

4. Oscillatory flow damping by a vertical magnetic field

The damping of the oscillatory flow by a vertical magnetic field is studied for the cavity with $A = 3$ for Gr = 150 000, by regularly increasing the Hartmann number Ha up to stabilization.

The results first show that stabilization is obtained for small values of Ha (Ha = 2.5), and that the decrease of fluctuations depends linearly on Ha. As Ha is increased, the time signals (given in Fig. 7 for the dimensionless temperature at the point ($x = 0.25$, $y = 0.25$, $z = 1.5$)) get gradually more simple, going through a double period signal at Ha = 1.25, before giving a purely periodic signal at Ha = 1.5 which persists with a decreasing intensity

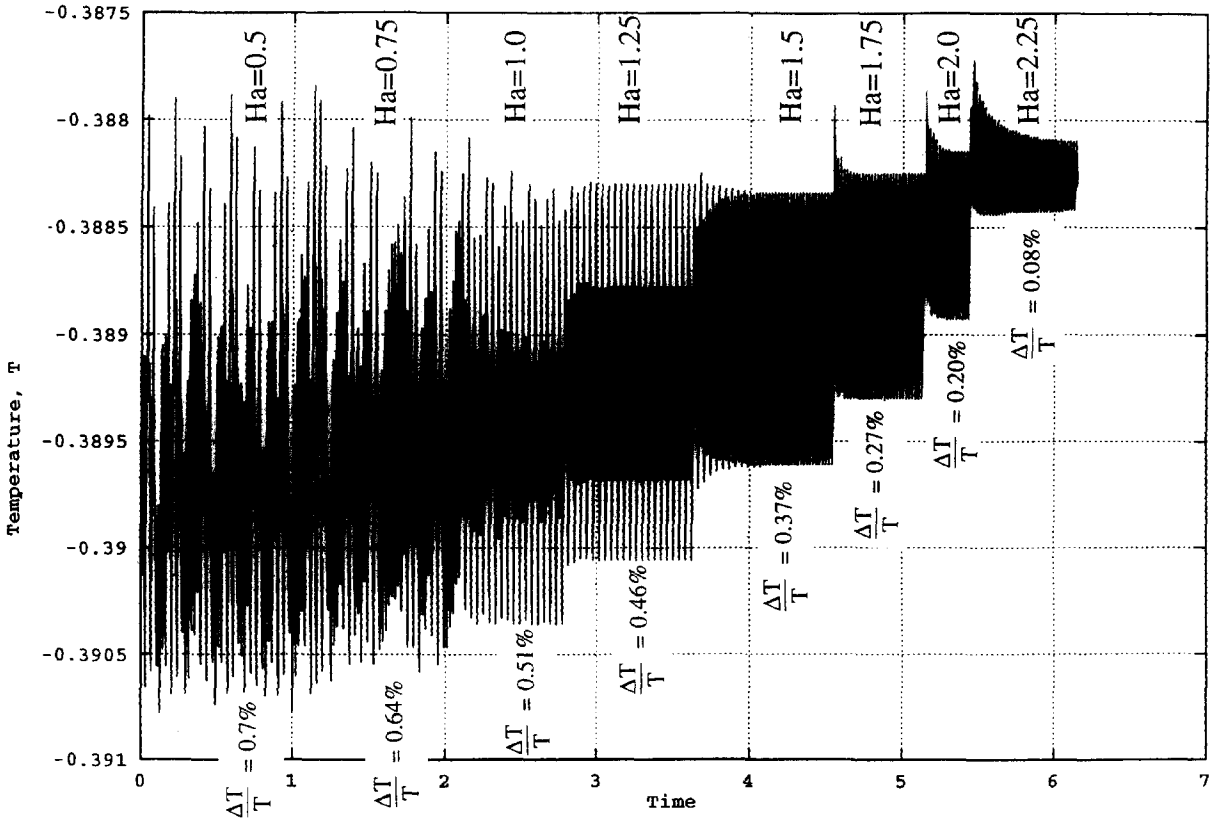

Fig. 7. Time series of the dimensionless temperature T at the point ($x = 0.25$, $y = 0.25$, $z = 1.5$) for increasing values of Ha; Gr = 1.5×10^5 and $A = 3$. ($\Delta T/T = (T_{max} - T_{min})/((T_{max} + T_{min})/2)$)

up to stabilization. The corresponding power spectra show the progressive disappearance of the low-frequency peaks ($f_0/2$ being the last to disappear), whereas the fundamental frequency f_0 is maintained with only a very small shift.

An interesting feature is that, during magnetic stabilization towards a steady flow, the original symmetry properties of the steady flow are not restored. Moreover, if Ha is then decreased, a periodic flow is again found as soon as Ha = 2.25, which does not give any evidence of a hysteresis phenomenon.

5. Conclusion

This study of oscillatory convection has shown that, for moderate length cylindrical cavities, the emerging instability corresponds to a shear stress instability (Helmolz instability) initiated at the centre of the cavity in the stagnation zone determined by the two end recirculation flows. This instability grows while being transported towards the end walls where it is damped. The instability affects mainly the longitudinal direction, as the reflexion symmetry with respect to the transverse middle axis is broken, while the reflexion symmetry with respect to the longitudinal middle plane is maintained. This main phenomenon corresponds to the fundamental frequency, but a low frequency is also obtained which is connected to the change in the position of the stagnation zone from one side of the transverse middle axis to the other.

The damping of these oscillations can be obtained by the action of a vertical magnetic field, and the magnetic field intensity necessary for this damping is quite small (stabilization obtained for Ha < 2.5). The first action of the magnetic field is to regularize the oscillations by suppressing the low frequencies until a mono-periodic signal of decreasing intensity is obtained. The stabilization leads to a steady flow, but this flow has not recovered the usual symmetries of the steady configuration.

Acknowledgements

We wish to thank Professor R. Moreau and Doctor L. Davoust from MADYLAM and Doctor J.P. Garandet from CEN Grenoble for helpful discussions. This work is supported by the "Centre National des Etudes Spatiales". The calculations were carried out on a Cray YMP C98 computer with the support of the CNRS through the "Institut du développement et des ressources en informatique scientifique" and on a SP2 parallel computer with the support of the CNUSC.

References

[1] D.T.J. Hurle, E. Jakeman, C.P. Johnson, J. Fluid Mech. 64 (1974) 565.
[2] S.M. Pimputkar, S. Ostrach, J. Crystal Growth 55 (1981) 614.
[3] M.C. Hung, C.D. Andereck, Subharmonic transitions in convection in a moderately shallow cavity, in: B. Roux (Ed.), Numerical Simulation of Oscillatory Convection in low-Pr Fluids, Notes on Numerical Fluid Mechanics, vol. 27, Vieweg, Braunschweig, 1990, pp. 338–343.
[4] J.M. Pratte, J.E. Hart, J. Crystal Growth 102 (1990) 54.
[5] A.E. Gill, J. Fluid Mech. 64 (1974) 577.
[6] J.E. Hart, J. Fluid Mech. 132 (1983) 271.
[7] P. Laure, B. Roux, C.R. Acad. Sci. Paris 305 (1987) 1137.
[8] M. Afrid, A. Zebib, Phys. Fluids A 2 (8) (1990) 1318.
[9] H. Ben Hadid, D. Henry, S. Kaddeche, J. Fluid Mech. 333 (1997) 23.
[10] H. Ben Hadid, D. Henry, J. Fluid Mech. 333 (1997) 57.
[11] H. Ben Hadid, D. Henry, J. Crystal Growth 166 (1996) 436.
[12] L. Davoust, Thesis, University of Grenoble, France, 1996.
[13] J. Baumgartl, G. Müller, Calculation of the effects of magnetic field damping on fluid flow- Comparison of magnetohydrodynamic models of different complexity, in: Proc. 8th European Symp. on Materials and Fluid Sciences in Microgravity (ESA SP-333), ESA Publ. Division c/o ESTEC, Noordwijk, The Netherlands, 1992, pp. 161–164.
[14] A.J. Patera, J. Comput. Phys. 54 (1984) 468.
[15] G.E. Karniadakis, M. Israeli, S.A. Orszag, J. Comput. Phys. 97 (1991) 414.